NIPES

Journal of Science and Technology Research

Journal homepage: www.nipesjournals.org.ng

A Comprehensive Pressure Distribution Model for Horizontal Well in a Gas-Cap Reservoir

[1]Ogbue M.C., [2]Anamonye G. U., [2]Aloamaka A., [1]Agbabi P. O., [3]Enyi L. C., [4]Adewole E.S., [4]Bello K.O.,

[1]Department of Petroleum Engineering, Delta State University, Abraka, Oleh Campus, Nigeria.
[2] Department of Electrical Engineering, Delta State University, Abraka, Oleh Campus, Nigeria.
[3]Department of Mechanical Engineering, Delta State University, Abraka, Oleh Campus, Nigeria.
[4]Department of Petroleum Engineering, University of Benin, Benin City, Nigeria.
Corresponding author: mogbue@delsu.edu.ng

Article Info

Keywords: *Horizontal well, gas cap, pressure distribution model, unlimited number of flow regimes.*

Received 11 March 2024
Revised 22 April 2024
Accepted 29 April 2024
Available online 20 May 2024

https://doi.org/10.5281/zenodo.11222168

Abstract

Subjecting well test data to interpretation model limits the data to capacity of the model. It is therefore necessary that pressure distribution models have all pertinent features that enhance accuracy of well test analyses. Flow regimes have been identified by the characteristic shape of their flow pattern. But the existing well test interpretation models limit the spatial orientation of these flow patterns within the three-principal axes of a reservoir. Thus, the number of flow regimes is limited. This article presents a comprehensive pressure distribution model for horizontal well in a reservoir subject to a gas cap. Pressure distribution in form of dimensionless pressure and dimensionless pressure derivatives were derived from Source and Green's functions. Result show that, the type of flow regime that would exist and its interval of existence are determined by the architecture of the reservoir system, reservoir system parameters and the fluid properties. Additional six flow regimes, which hitherto were not considered, have been presented. Each flow regime was characterized by its flow pattern, its spatial orientation in relation to the three-principal axes, its interval of existence and characteristic signature on log-log pressure distribution plot. It was observed that boundary dominated effect of gas cap resulted in constant value of dimensionless pressure and a declining value of dimensionless pressure derivative.

1.0. Introduction

Predisposition of publications is to focus on successful applications. However, predictions of performance of well are perturbed by significant amount of uncertainties. These failures occurred in spite of cautious and detailed reservoir evaluation work [1]. It therefore suggests that the thoroughness of reservoir evaluation work may not be the problem. Rather, the problem might have been from the model used for such predictions. Subjecting well test data to interpretation model limits the data to capacity of the model. It is therefore necessary that pressure distribution models have all pertinent features that enhance accuracy of well test analyses. Various studies have been developed by several researchers in determining the transient flow behavior of horizontal wells. Emphasis was on pattern of flow has been amply treated. Elliptical flow which was not initially included as one of existing flow regime has been explained and its application established [2].

Abounding articles on solutions of pressure distribution of horizontal well suggests that there is sufficient knowledge on horizontal well hydraulics. However, limitation of flow regimes to conventional few prevailed. With the more recent years, analytical solutions for some flow regimes such as hemispherical flow, spherical flow, radial flow, has been provided in literature [2, 3, 4, 5, 6]. At least, flow regimes have been identified by their characteristic shape of flow pattern. But these patterns are not spatially restricted to a particular direction. If analyses of horizontal well hydraulics is extended to geological facts, the spatial orientation of these flow pattern can change within the three-dimensional space of a reservoir system. By relaxing some limiting assumptions the facts becomes obvious. For instance, radial flow which is usually treated as a single flow regime existing only in x-y-axes can be observed in x-z axes, as well as y-z axes. It is plausible because dynamics of the reservoir fluid is not controlled by the geometry of reservoir system only. Rather, dynamics of reservoir fluid is also controlled by properties of the fluid and petrophyical properties of the reservoir rock. Put in a different light, if the order of magnitude of permeability along the principal axes is rearrange, the flow pattern would develop but its spatial orientation along the x,y,z-axes would change, even without changing the reservoir dimensions or the architecture of the reservoir system. In this article, flow regimes are presented not only by the characteristic pattern of flow but also by the spatial orientation of the pattern of flow along the three- dimensional axes. Flow regimes are presented to be determined not only by geometry of the reservoir system, but also determined by the permeability of reservoir and fluid properties as well. Also, correlation for determining starting time and ending time of each flow regimes will be considered. Defining the accurate starting and ending times of the different flow regimes is a drawback of the conventional technique. Back in time, new flow periods (regimes) were identified by using new solutions approach to pressure distribution of horizontal wells in reservoirs and by considering real conditions. [7]. Type-curve matching requires that all flow regimes must be present so as to obtain unique answers. A technique to interpret horizontal well pressure data without resorting to type-curve matching was introduced in 1996 [8]. In that study, however, the elliptical-flow regime, in spite of its usefulness was not included. In this article, the elliptical-flow regime is considered among others flow regime which are hitherto not considered. The proposed methodology will be verified by means of the analysis with examples reported in the literature. It is important to explore other available options, not just for the sake of having variety, but to be able to meet the need for cases where original design of reservoir system changed due to contingencies. For instance, the design of fracture caused by hydraulic fracturing have been observed to change from vertical direction to horizontal direction in tectonically active reservoirs, shallow reservoirs and abnormally high-pressure reservoirs, [9, 10, 11, 12, 13]. In situation where well intersects a natural fracture, the specific orientation of the fracture plane with respect to the wellbore is not certain [14]. Transient pressure behavior is required in these wells both for production forecast and fracturing design [15]. But proper transient behavior cannot be obtained if model applied is insufficient.

2. 0 Methodology

In chronological order, procedure involved conceptual model, physical model, mathematical model and analyses of results.

2.1 Conceptual Model

The conceptual model will help to relax existing assumptions that create restriction in the flow regimes considered. Consider a horizontal well in a cuboid reservoir overlaid by a gas cap. Dynamics of fluid in the reservoir is controlled by the properties of the fluid, petrophysical properties of the reservoir rock and the geometry of reservoir system. There is no prescribed order of magnitude of permeability along the major axes.The permeability along these main axes are, k_x, k_y and k_z representing the permeability along x-axis, z-axis and z-axis respectively.

2.2 Physical Model

A two-dimensional schematic of the physical model is presented in Figure 1.

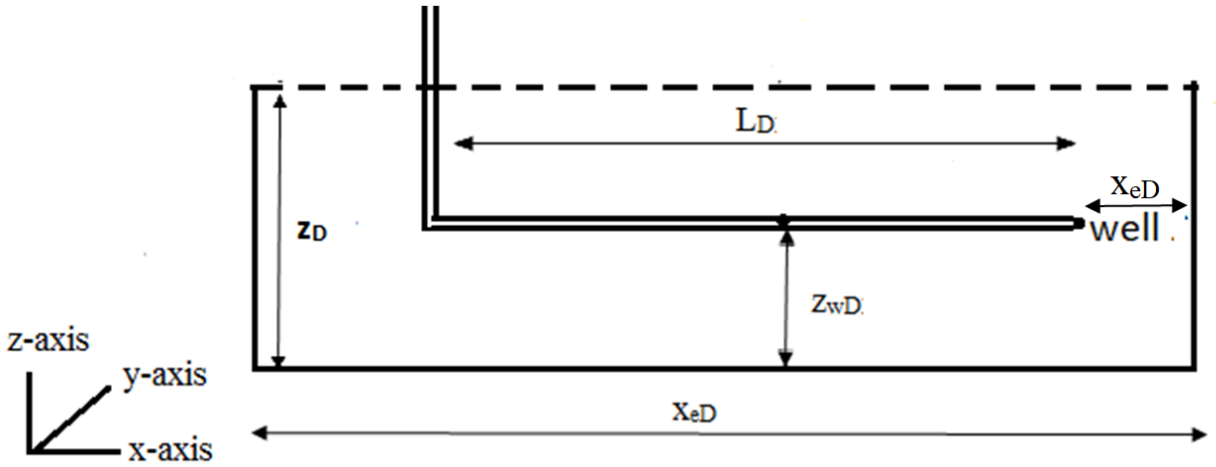

Figure 1: Two-dimensional schematic of the Physical Model of Horizontal Well in a Reservoir Subject to Bottom Water.

Assumptions:

(1) All external boundaries are closed except for the top which is bounded by gas cap (2) The reservoir contains a single-phase (3) The reservoir is horizontal and its thickness is uniform

2.3 Portrayal of all the Possible Flow Regime

The possible fluid flow patterns of a horizontal well in a cuboid reservoir and their spatial orientation along the principal axes are presented. Portrayal of the entire possible flow regime is presented under the following steps: flow patterns, spatial orientation, conditions of existence and interval of existence. Rationales on the specific approach used to derive each step are detailed thus:

1. Flow patterns were adopted as established in the literature based on empirical observations [2, 3, 5. 6, 7, 15, 16, 17].
2. Spatial orientations adopted derived from the Physical Model established in Section 2.2. Spatial orientations of these patterns for each flow regime were chosen by considering other possible axial orientations, instead of limiting the pattern to only one spatial orientation, as seen in literature. Such limitation found in literature will not exist if the Conceptual Model established in Section 2.1, was adopted.
3. Conditions for existence were established based on logical conclusions derived from knowledge of reservoir flow regimes [7, 16, 17], the Physical Model in Section 2.2., and Odeh et al. strategy [16].
4. Interval of existence for each of the identified flow regimes were established as an extension of analytical solutions provided in strategy of Odeh and Babu [16], bearing Rationale (1) and Rationale (2) in mind.

Furthermore, knowledge of geometry of the reservoir system, the permeability of reservoir and fluid properties are employed in describing the dynamics of fluid. The conditions that enable their existence are also provided. Each flow regime is characterized by its flow pattern, its spatial orientation in relation to the three-principal axes, its clearly defined interval of existence and characteristic signature on log-log pressure distribution plot. Table 1 is a list of all the possible flow regimes and summary of their features.

Table 1: List of possible flow regimes with description of their flow pattern, condition of existence and interval of existence

Label	Description of Flow Pattern	Condition of Existence	Interval of Existence
ER_{yz}	Circular along y, z-axes.	Flow is within well along x-axis	0 - t_{D1}
EE_{xyx}	Ellipsoidal along x, y, z-axes	Flow is beyond tips of well along x-axis	$t_{D2} - t_{D3}$
EL_y	Linear along y-axis.	Only bottom of z-axis is felt given ER_{yz} preceded	$t_{D4} - t_{D5}$
EL_z	Linear along z-axis.	y-axis is felt given ER_{yz} preceded	$t_{D6} - t_{D7}$
PR_{xy}	Circular along along x, y-axes	Given EL_y, EE_{xyz} preceded but only bottom of z-axis felt	$t_{D8} - t_{D9}$
PR_{xz}	Circular along along x, z-axes	Given EL_z, EE_{xyz}, preceded but y-axis felt	$t_{D10} - t_{D11}$
PR_{yz}	Circular along along y, z–axes	Given EE_{xyz} preceded but x-axis felt	$t_{D12} - t_{D13}$
LL_x	Linear along x-axis	Given PR_{xy} and y-axis felt or PR_{xz} and only bottom of z-axis felt or EE_{xyx} and y-axis , only bottom of z-axis felt	$t_{D14} - t_{D15}$
LL_y	Linear along y-axis	Given PR_{xy} and x-axis felt or PR_{yz} and only bottom of z-axis felt or EE_{xyx} and x-axes , only bottom of z-axis felt	$t_{D16} - t_{D17}$
LL_z	Linear along z-axis	Given PR_{xz} and x-axis felt or PR_{yz} and y-axis felt or EE_{xyx} and x,y-axes felt	$t_{D18} - t_{D19}$
BD	Along x, y, z-axes	All boundaries felt or only top of z-axis	$t_{D20} - t_{Del}$

2.4 Mathematical Model

Mathematical model developed from the physical model. It is the actual pressure distribution. It is in form of dimensionless pressure, P_D, and dimensionless pressure derivative, P'_D, as functions of reservoir system parameters and fluid properties. Mathematical model was derived from instantaneous Source and Green's functions [18].

2.4.1. Description along each Principal Axis

Description of reservoir system along each axis is necessary for suitable selection of the functions.

a. Description along x- axis:

Schematic of model along x- axis is as shown in Figure 2.

Figure 2: Schematic of model along x-axis.

i. Both ends of the reservoir are circumscribed.
ii. Well length coincides with the x-axis
iii. Therefore, the well is an infinite slab source in an infinite slab reservoir.

iv. Source number is x (x).

b. Description along y-axis:

Schematic of model along y-axis is as shown in Figure 3.

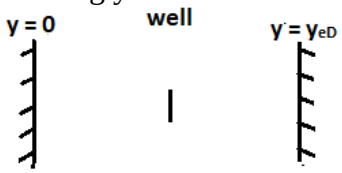

Figure 3: Schematic of model along y-axis.

i. Both ends of the reservoir are circumscribed
ii. Well length does not coincide with the y-axis
iii. Therefore, the well is an infinite plane source in an infinite slab reservoir.
iv. Source number vii(y).

c. Description along z-axis:

Schematic of model along z-axis is as shown in Figure 4.

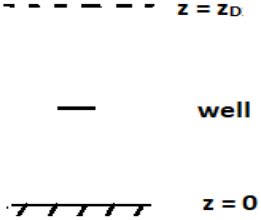

Figure 4: Schematic of model along z-axis

i. The reservoir is circumscribed at the bottom, but permeable at the top.
ii. Well length does not coincide with the z-axis.
iii. Therefore, the well is an infinite plane source in an infinite slab reservoir.
iv. Source number ix (z).

2.4.2 Mathematical Model in form of Dimensionless Expression

The appropriate Source and Green' functions in their dimensionless pressures and dimensionless pressure derivative were written using Newman product rule:

$$P_D = 2\pi h_D \int_0^{t_D} x(x).vii(y).ix(x)d\tau \quad (1)$$

Equation 2 is the late time dimensionless expression. Before late time, series of possible flow regime occurred.

Dimensionless pressure at any time of interest is a time superimposition of individual flow regimes that have existed up to that time of interest. Each flow regime is represented by an integrand, and the limits of the integration are the interval of its existence. So, Equation 1 can be written as Equation (2) showing for all possible flow regimes.

$$P_D = 2\pi h_D \int_0^{t_{D1}} ii(x).i(y).i(z)d\tau + 2\pi h_D \int_{t_{D2}}^{t_{D3}} ii(x).i(y).i(z)d\tau + 2\pi h_D \int_{t_{D4}}^{t_{D5}} ii(x).i(y).ix(z)d\tau + 2\pi h_D \int_{t_{D6}}^{t_{D7}} ii(x).vii(y).i(z)d\tau + 2\pi h_D \int_{t_{D8}}^{t_{D9}} ii(x).i(y).ix(z)d\tau + 2\pi h_D \int_{t_{D10}}^{t_{D11}} ii(x).vii(y).i(z)d\tau + 2\pi h_D \int_{t_{D12}}^{t_{D13}} x(x).i(y).i(z)d\tau + 2\pi h_D \int_{t_{D14}}^{t_{D15}} ii(x).vii(y).ix(z)d\tau + 2\pi h_D \int_{t_{D16}}^{t_{D17}} x(x).i(y).ix(z)d\tau + 2\pi h_D \int_{t_{D18}}^{t_{D19}} x(x).vii(y).i(z)d\tau + 2\pi h_D \int_{t_{D20}}^{t_{Del}} x(x).vii(y).ix(z)d\tau \quad (2)$$

And the dimensionless pressure derivative as shown in Equation 3 and 4

$$P'_D = \frac{\partial P_D}{\partial ln t_D} \quad (3)$$

$$P'_{D2} = 2\pi h_D\{[ii(x).i(y).i(z)] + [ii(x).i(y).i(z)] + [ii(x).i(y).ix(z)] + [ii(x).viii(y).i(z)] + [ii(x).i(y).ix(z)] + [ii(x).vii(y).i(z)] + [x(x).i(y).i(z)] + [ii(x).vii(y).ix(z)] + [x(x).i(y).ix(z)] + [x(x).vii(y).i(z)] + [x(x).vii(y).ix(z)]\} \quad (4)$$

Each flow regime is identified mathematically by its unique: (1) Source functions (2) interval of existence (limits of integration). No two flow regimes have the same Source functions and interval of existence (limits of integration. If production continues beyond t_{D20}, then t_{Del} is the end of economic production (economic limit) of the well.

2.4.3 Delineation of Flow Regimes

Modified form of correlation by Odeh and Babu was used to delineate the intervals of subsistence of each flow regime [16].

Limits of integration shown in Equations 3 which represent intervals of existence of each flow regime were estimated by correlations presented in Table 2.

Table 2: Interval of Flow Regimes

Regime	Interval of Existence	
	Starting Time	**Ending Time**
ER_{yz}	0	t_{D1}= *min. 0.132, $\frac{1.9008d_{zD}^2}{L_D^2}$, $\frac{1.7424d_{yD}^2}{L_D^2}$
EE_{xyx}	t_{D2}= 0.132, provided $\frac{1.9008d_{zD}^2}{L_D^2}$ & $\frac{1.7424d_{yD}^2}{L_D^2}$ > 0.132	t_{D3}= min. $\frac{1.9008d_{zD}^2}{L_D^2}$, $\frac{1.7424d_{yD}^2}{L_D^2}$, $2.112\left(\frac{d_{xD}}{L_D}+\frac{1}{4}\right)^2$
EL_y	t_{D4}= $\frac{1.9008d_{zD}^2}{L_D^2}$,provided $\frac{1.9008d_{zD}^2}{L_D^2}$ < 0.132, $\frac{1.7424d_{yD}^2}{L_D^2}$	t_{D5}= min 0.16896, $\frac{1.7424d_{yD}^2}{L_D^2}$
EL_z	t_{D6}= $\frac{1.7424d_{yD}^2}{L_D^2}$ provided $\frac{1.7424d_{yD}^2}{L_D^2}$ < 0.132, $\frac{1.9008d_{zD}^2}{L_D^2}$	t_{D7}= min 0.16896, $\frac{1.9008d_{zD}^2}{L_D^2}$
PR_{xy}	t_{D8}= 1.56288	t_{D9}= min$\frac{1.7424d_{yD}^2}{L_D^2}$, $2.112\left(\frac{d_{xD}}{L_D}+\frac{1}{4}\right)^2$
PR_{xz}	t_{D10}= 1.56288	t_{D11}= min. $\frac{1.9008d_{zD}^2}{L_D^2}$, $2.112\left(\frac{d_{xD}}{L_D}+\frac{1}{4}\right)^2$
PR_{yz}	t_{D12}= 1.56288	t_{D13}= min $\frac{1.9008d_{zD}^2}{L_D^2}$, $\frac{1.7424d_{yD}^2}{L_D^2}$
LL_x	t_{D14}= min. $\frac{1.9008d_{zD}^2}{L_D^2}$, $5.068\left(\frac{d_{xD}}{L_D}+\frac{1}{4}\right)^2$	t_{D15}= $\frac{1.7424d_{yD}^2}{L_D^2}$
LL_y	t_{D16}= min. $\frac{1.7424d_{yD}^2}{L_D^2}$, $5.068\left(\frac{d_{xD}}{L_{D1}}+\frac{1}{4}\right)^2$	t_{D17}= $\frac{1.9008d_{zD}^2}{L_D^2}$
LL_z	t_{D18}= min. $\frac{1.7424d_{yD}^2}{L_D^2}$, $\frac{1.9008d_{zD}^2}{L_D^2}$	t_{D19} = $5.068\left(\frac{d_{xD}}{L_D}+\frac{1}{4}\right)^2$
BD	t_{D20} = **max. $\frac{1.7424d_{yD}^2}{L_D^2}$, $\frac{1.9008d_{zD}^2}{L_D^2}$, $5.068\left(\frac{d_{xD}}{L_D}+\frac{1}{4}\right)^2$	t_{Del}

*min. denotes “minimum of” **max. denotes “maximum of”

3.0 Results and Discussion

The first step was verification of model, followed by analyses of results.

3.1 Verification of Model

Models from literature were used to verify this model. The verification was done in segments, because the model of this article is complex and no single model in literature can adequately be used to verify it. Each segment of verification was done by comparing some parts of this model of this work with model in other literature that has similar case in point.

Example 1: This segment of verification was done with model of Goode et al. [17] data used are as shown in Table 3.

Table 3: Reservoir System Parameters used for Verification of Model using Goode's et al model [17]

Parameter	K_x, md	K_y, md	K_z, md	Q, bbl/day	μ, cp	r_w(ft)	h_x, ft
Value	50	100	25	3000	1.5	0.354	13500
Parameter	B_o, bbl/STB	h_y, ft	L. ft	∅, %	C_t, psi^{-1}	h_z, ft	
Value	1.5	30	1000	10	$3.0x10^{-5}$	60	

As shown Table 3, permeability values along the three principal axes are close values. But the value of permeability along y-axis is highest, followed by permeability along x-axis is highest, and permeability along z-axis is the least. The dimensions of the reservoir along the three principal axes are close values. But the dimensions of the reservoir along x-axis is highest, followed by permeability along z-axis is highest, and permeability along y-axis is the least. Also, the well length is short compared to length of the reservoir. Using definition of dimensionless values in equations 5 to 21, data given in Table 3 were converted to dimensionless parameters. The pressure distribution was plotted on a log-log graph as shown in Figure 5.

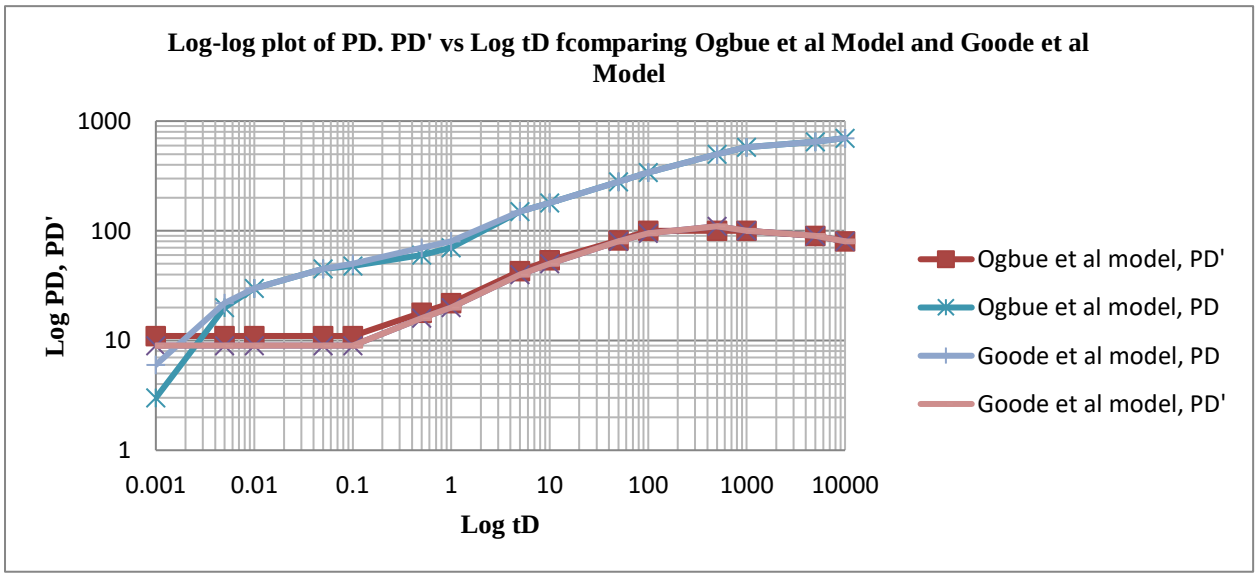

Figure 5: Log-log plot of P_D, P_D' versus t_D for validation of Ogbue et al model using Goode et al model

As shown in Figure 5, early time radial flow, ER_{yz}, , t_D = 0.005 to 0.1. P_D rose with time, P_D' was constant. It stopped when flow was beyond the tips of the well. Since well length was short compared to length of reservoir along x-axis, flow will certainly be beyond the tips of the well in a short time. Ellipsoidal flow, EE_{xyx}, could easily have developed.. But there is much closeness between the well and the boundary along y-axis. Also, there is high permeability along y-axis.

Condition like that will make boundary along y-axis to be felt much earlier than other boundaries. In this manner, development of elliptical flow and its characteristic signatures on log-log plot of P_D' was masked. Hence, y-axis was felt at about $t_D = 0.1$. As y-axis is a closed boundary, P_D and P_D' simultaneously rose with time indicating the characteristic signature of linear flow, LL_x. At tD = 100, boundary along z-axis was felt. The z-axis has a constant pressure boundary at the top. So, P_D was observed to be constant while P_D' gradually decrease as it tends to zero. Similar trend was observed in work of Li Chen [4] were crossflow from another layer created a constant a constant pressure boundary. So, P_D was observed to be constant as the plot straighten horizontally, while P_D' gradually decrease as it tends to zero.
Curve obtained from Ogbue et al model compares well with Goode et al model, though higher values of P_D, were obtained at some point. There were points along the curve P_D'where Goode's model resulted in higher values.

Example 2: Comparison was further done between the model of this study and with model of Mutisya et al [19]. The parameters in dimensioned form are shown in Table 4,.

Table 4: Reservoir System Dimensioned Parameters of Mutisya et al model [19] used for Validation of Model

Case	L. ft	x_w, ft	y_w, ft	z_w, ft	Z, ft	x_e, ft	y_e, ft	z_e, ft	h, ft
A	5000	134	200	160	160.5	6000	400	200	200
B	3500	134	200	160	160.5	6000	400	200	200
	dx, ft	dy, ft	dz, ft	Dx, ft	Dy, ft	Dz, ft	K_x, md	K_y, md	K_z, md
A	134	200	160	634	201	161	22	16	20
B	134	200	160	634	201	161	22	16	20

For Case A and Case B, the axial permeability values are very close to each other, although $K_x > K_z > K_y$. Although, the values of reservoir dimensions are very close for y-axis and z-axis, the values of reservoir dimensions along x-axis is several folds higher than the others, $x_e >> y_e >. z_e$. The closest distance from tip of the well to the boundary of reservoir was observed to be along x-axis, followed by distance along y-axis, lastly distance along y-axis.
Dimensionless parameters of reservoir system was obtained using equations 5 to 21. Dimensionless parameters are shown in Table 5.

Table 5: Reservoir System Dimensionless Parameters used for Validation of Model using Mutisya et al model [19]

Case	L_D	x_{wD}	y_{wD}	z_{wD}	x_{eD}	y_{eD}	z_{eD}	h_D,
A	1.1669	0.5	0.8757	0.6266	22.404	1.7514	0.7832	0.7832
B	8.1681	0.5	0.1251	0.0056	3.1206	0.2502	0.028	0.1119
	x_D	y_D	z_D					
A	0.5	0.8757	0.6285					
B	0.5	0.1251	0.0059					

As observed, for x-axis the permeability is not much higher than other and distance of boundary to tip of the well is shorter than distances of other boundaries to tip of well. It is would take a shorter time before boundary along x-axis is felt if the flow initially within the well would quickly get beyond the tip of the well. However it will take some tip before flow goes beyond the tips of the well. The well length is long compared to length of the reservoir. Therefore, flow will certainly not get beyond the tips of the well in a short time. Such condition will make boundary along z-axis to be felt earlier than other boundaries, because permeability along z-axis is about the value with others but its boundary is closest to the tip of the well.

Therefore, boundary along y-axis would be felt almost immediately after z-axis and boundary along x-axis much later. But boundary dominated effect of z-axis will mask their effect. Boundary dominated effect of z-axis is a constant pressure boundary supported by gas cap.

.

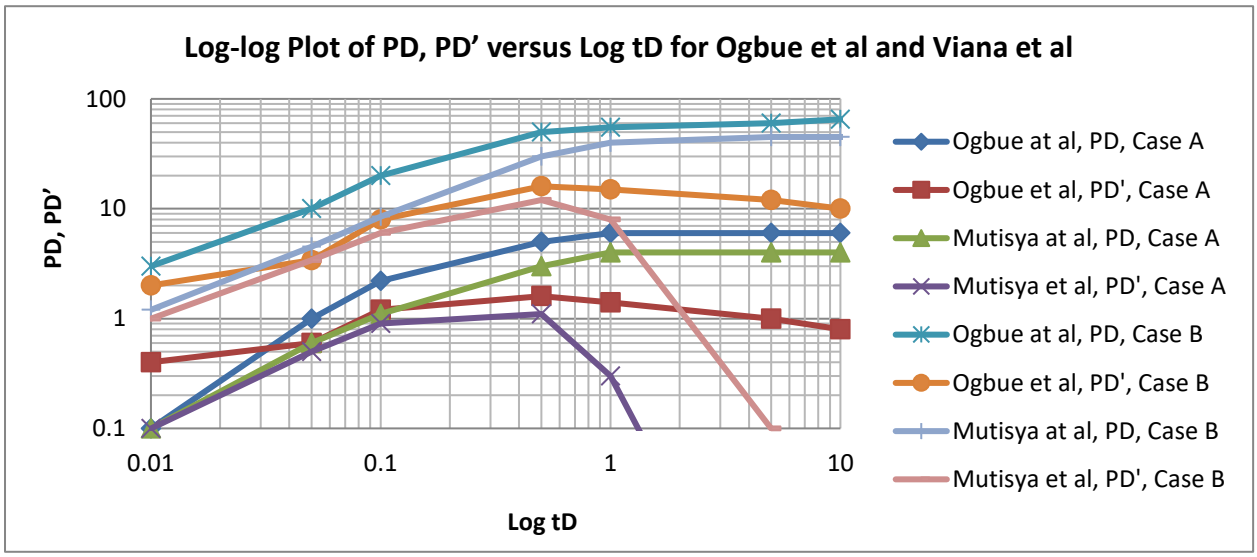

Figure 6: Comparison with the results from Ogbue et al model and Mutisya et al model on log-log plot.

As shown in Figure 6, early time radial flow, ER_{yz}, was short lived, t_D = 0.01 to 0.05. it stopped when flow got to boundary along z-axis. As shown, boundary dominated flow regime, BD, established very early, t_D = 0.05, due to the conditions of z-axis explained earlier. The characteristic signatures on log-log plot of P_D, P_D' vs t_D was shown. P_D, tended to a constant value with time, while PD' sloped downwards towards zero. The higher permeability along y-axis could not compensate for the farther distance of its boundary to well, hence y-axis was not felt earlier than z-axis. The closeness of the boundary along x-axis to the well could not compensate for the permeability, hence y-axis was not felt earlier than z-axis. Thus, it establishes the fact that dynamics of fluid is controlled jointly by reservoir geometry and petrophysical property of the reservoir. Curve obtained from Ogbue et al. model compares well with Mutisya et al model [19], though higher values of P_D, P_D' were obtained at some point. There were points along the curve where Mutisya model resulted in lower values.

3.2 Possible Flow Regime of Horizontal Well in Reservoir Supported by Gas Cap.

Comprehensive list of all possible flow regimes and their intervals of subsistence are presented in Table 1 For any given set of data, the flow regime that subsisted, can be identified by (1) its characteristic signature on the log-log plot of dimensionless pressure and it dimensionless pressure derivative (2) Table 1 (3) Analyses derived from the reservoir system parameters. Correlation given in Table 2 can also be used to define the interval of subsistence. When the starting time is higher than the ending time, the flow regime does not exist. Also, some flow regime does not exist in particular set of parameters if certain flow regimes precede them. Some flow regimes obliterate others owing to the reservoir configuration. It means also that some flow regimes cannot co-exist. In some instances, where two consecutive flow regime overlap, i.e. another flow regime starts when other has not fully died developed, only the fully developed would subsist while the other would be masked.

3.2.1 Description of the Individual Flow regimes

All flow regimes cannot exist in one flow period even if they are possible flow regimes. Here are the possible flow regimes and their description.

1. ER_{yz} : This flow is radial along y, z – axes but contained within the well length and aligned along the x-axis. This flow is an early radial flow regime around the well length, provided flow has not gone beyond tip of well. During this time, flow along x – axis is not affected by time as flow is still within the wellbore. This flow regime will stop when flow is beyond tips of the well or when any of the external boundaries is felt. During this time of subsistence, dimensionless pressure rises moderately with respect to dimensionless time. The slope of the log –log plot for the pressure is constant. Dimensionless pressure derivative is constant.
2. EE_{xyx} : During this regime, flow is along x, y, z –axes. It starts if there is sufficient time for flow to go beyond the tips of the well before any boundary is felt. This flow pattern is a ellipsoidal forming an envelope around the length of the well. It occurs if well length is short compared to distances between the well and boundaries along any axis. It can also occur if permeability along the axis of length of well is comparatively higher than permeability along other axes. The dimensionless pressure rises very sluggishly with time while the dimensionless pressure derivative rises very moderately with time. It can be a symptomatic tool that suggests the need to extend producing well length.
3. EL_y: . Flow along y – axis. It occurs when the bottom boundary along z – axis is felt first before other boundaries. It is possible when reservoir extent is closer along z – axis or the permeability along that axis is relatively high. It obliterates ellipsoidal flow if it occurred. The dimensionless pressure and the dimensionless pressure derivative rises rapidly
4. EL_z: Flow along z – axis. It occurs when bounded bottom boundary has been felt. It occurs if the reservoir thickness is low compared with other dimensions of the reservoir or vertical permeability is relatively high. The dimensionless pressure and the dimensionless pressure derivative rises rapidly When the constant pressure top is felt, it leads to boundary dominated flow which will be discussed later. In such case, the dimensionless pressure is tends to straighten horizontally, while the dimensionless pressure derivative declines rapidly and tends towards zero thus indicating external energy. It obliterates spherical flow if it occurred
5. PR_{xy}: Radial flow along x, y –axes. The flow pattern is radial at the top to bottom of well. The dimensionless pressure tends to a constant value, while the dimensionless pressure derivative declines as it tends to zero.
6. PR_{xz}: Radial flow along x, z – axis. This is Pseudo radial flow regime. The flow pattern is radial at the sides of the well. It is not as the real radial flow at early time because it is observed after boundary has been felt and effect of boundary has commenced. The dimensionless pressure tends to a constant value, while the dimensionless pressure derivative declines as it tends to zero.
7. PR_{yz}: Radial flow along y, z – axis. This is given Pseudo radial flow regime. The flow pattern is radial at around the length of the well. The dimensionless pressure tends to a constant value, while the dimensionless pressure derivative declines as it tends to zero.
8. LL_x: Flow along x –axis. The flow is late time linear flow. The dimensionless pressure is tends to rise rapidly, while the dimensionless pressure derivative also rises rapidly
9. LL_y: Flow along y – axis. The flow is late time linear flow. The dimensionless pressure and its rises rapidly indicating completely sealed boundary.
10. LL_z: Flow along z – axis. At least boundaries along two axes have been felt. Another linear flow, late time linear flow, is observed. If only the bottom is felt, the dimensionless pressure and the dimensionless pressure derivative rises rapidly indicating sealed boundary. If the top boundary is felt, the dimensionless pressure tends to constant value and its derivative declines towards zero indicating constant pressure boundary.

11. BD: All boundary felt or the top boundary has been felt. Effect of constant pressure boundary is felt. The dimensionless pressure tends to constant value and its derivative declines towards zero indicating completely constant pressure boundaries because of effect of constant pressure boundary.

From the foregoing, the various factors considered can be categorized into three classes of variables: (1) Design and parameters of the reservoir system (2) reservoir characterization (3) subsisting flow regimes under the certain conditions. If two are known, they can be used to determine the third. We can study these instances if we consider three different scenario tagged Case 1, Case 2 and Case 3.
Case 1: If the subsisting flow regimes are unknown, but design and parameters of the reservoir system as well as reservoir characterizations are known. The subsisting flow regimes during flow conditions can be determined by matching with type curve or interpreting pressure/pressure derivative plot with time in relation to given parameters of reservoir system.
Case 2: if reservoir characterization is the unknown, design of the reservoir system can be done to favour desired flow regimes, theoretical results can then be used to verify the field result, thus reservoir characterization can be achieved.
Case 3: This is actually field development strategy. If design and parameters of the reservoir system is unknown but reservoir characteristics and there are desired flow regimes are known. Given the reservoir characteristics and conditions that encourage existence of certain flow regimes, the design and choice of reservoir system parameters can be done to favour existence of the desired flow regimes. After several simulations the optimum design can be achieved.

Conclusion

A comprehensive pressure distribution of horizontal well in a reservoir subject to bottom water has been presented in form of mathematical model. Many observations have been discussed. This article can therefore, be concluded thus:

1. The type of flow regime that would exist and its interval of existence are determined by the architecture of the reservoir system, reservoir system parameters and the fluid properties.
2. Model was witnessed to have produced series of linear and radial. Flow patterns were aligned along any of principal axis or combinations of any of the three principal axes. Each flow regime could be recognized by its characteristic signature in the log-log graph plots of the pressure, pressure derivative versus time, geometry of reservoir system and the petrophysical properties of the reservoir.
3. Additional six flow regimes which hitherto were not considered have been presented. In all, eleven flow regimes have been studied in this work.
   Correlation for demarcating interval of flow regime has been extended to cater for the new flow regimes. The interval of existence depends on the reservoir system parameters. Existence of some flow regimes obliterates other flow regimes. Also, when the interval of subsistence is short, the flow regime is masked and not observed.

Acronyms

ER Early radial
EE Early Ellipsoidal
EL Early linear
PR Pseudo radial
LL Late linear
BD Boundary dominated

Subscript

x along x-axis
y along y-axis
z along z-axis
xy along x and y-axes
xz along x and z-axes

yz along y and z-axes
D dimensionless
e extremity of reservoir
w well
el economic limit

Nomenclature

S Source and Green's function
B oil volumetric factor, rbbl/STB
C_t total compressibility, psi^{-1}
i principal axis x, y, or z
h formation thickness, ft
k average geometric permeability, md
k_i formation permeability in the ith axis, md
L total length of horizontal well, ft.
Δp pressure drop, psi
P pressure, psi
P' pressure derivative, psi/hr
x_e dimension of reservoir along x-axis
y_e dimension of reservoir along y-axis
z_e dimension of reservoir along z-axis
z_w distance between the external wall of well and the bottom/top of the reservoir
d_x shortest distance between the tip of the well and boundary of the x −axis, ft
d_y shortest distance between the well and boundary of the y −axis, ft
d_z shortest distance between the external wall of well and boundary of the z −axis, ft
D_x longest distance between the tip of the well and boundary of the x −axis, ft
D_y longest distance between the well and boundary of the y −axis, ft
D_z longest distance between the external wall of well and boundary of the z −axis, ft
t time, hours
q flow rate, bbl/day

Greek Symbols

ϕ porosity, fraction
μ reservoir fluid viscosity, cp
τ dummy variable of time

Dimensionless Parameters

$$P_D = \frac{kh\Delta P}{141.2q\mu B_0} \quad (5)$$

$$k = \sqrt[3]{k_x k_y k_z} \quad (6)$$

$$h_D = \frac{2h}{L}\sqrt{\frac{k}{k_z}} \quad (7)$$

$$L_D = \frac{L}{2h}\sqrt{\frac{k_x}{k}} \quad (8)$$

$$x_D = \frac{2x}{L}\sqrt{\frac{k}{k_x}} \quad (9)$$

$$x_{eD} = \frac{2x_e}{L}\sqrt{\frac{k}{k_x}} \quad (10)$$

$$x_{wD} = \frac{2x_w}{L}\sqrt{\frac{k}{k_x}} \quad (11)$$

$$y_D = \frac{2y}{L}\sqrt{\frac{k}{k_y}} \quad (12)$$

$$y_{eD} = \frac{2y_e}{L}\sqrt{\frac{k}{k_y}} \quad (13)$$

$$y_{wD} = \frac{2y_w}{L}\sqrt{\frac{k}{k_y}} \quad (14)$$

$$z_D = \frac{2z}{L}\sqrt{\frac{k}{k_z}} \quad (15)$$

$$z_{eD} = \frac{2z_e}{L}\sqrt{\frac{k}{k_z}} \quad (16)$$

$$z_{wD} = \frac{2z_w}{L}\sqrt{\frac{k}{k_z}} \quad (17)$$

$$d_x = D_x = \frac{x_e - L}{2} \quad (18)$$

$$r_{wD} = \frac{z_{eD}}{2} - z_{wD} \quad (19)$$

$$t_D = \frac{0.001056kt}{\phi\mu C_t L^2} \quad (20)$$

$$x_w = \frac{x_e - L}{2} \quad (21)$$

Appendix 1

Basic instantaneous source functions (Courtesy of Gringarten A.C. and Ramey H.J.Jr., Society of Petroleum Engineers Journal, vol. 13,page 289-290, 1973)

X=0 Xw Xe	SOURCE	FUNCTION NUMBER	SOURCE FUNCTION
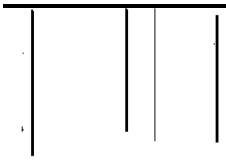	INFINITE PLANE SOURCE	I(X)	$\frac{exp\left[-\frac{(x-x_w)^2}{4n_x t}\right]}{\sqrt[2]{n_x t}}$
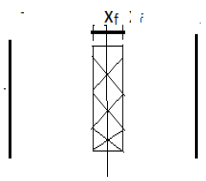	INFINITE SLAB SOURCE	II(X)	$\frac{1}{2}\left[erf\frac{\frac{x_f}{2}+(x-x_w)}{\sqrt[2]{n_x t}} + erf\frac{\frac{x_f}{2}-(x-x_w)}{\sqrt[2]{n_x t}}\right]$
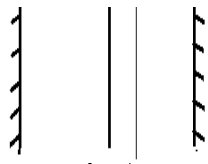	PRESCRIBED FLUX, PLANE SOURCE	VII(X)	$\frac{1}{x_e}\left[1+2\sum_{n=1}^{\infty} exp\left(-\frac{n^2\pi^2 n_x t}{x_e^2}\right)cos\frac{n\pi x_w}{x_e}cos\frac{n\pi x}{x_e}\right]$
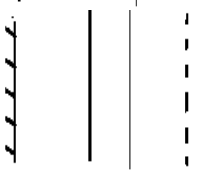	MIXED BOUNDARY, PLANE SOURCE	IX(X)	$\frac{2}{x_e}\sum_{n=1}^{\infty} exp\left(-\frac{(2n+1)^2\pi^2 n_x t}{4x_e^2}\right)cos\frac{(2n+1)\pi x_w}{x_e}cos\frac{(2n+1)\pi x}{x_e}$

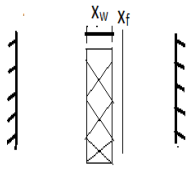	PRESCRIBED FLUX, SLAB SOURCE	X(X)	$\frac{x_f}{x_e}\left[1+\frac{4x_e}{\pi x_f}\sum_{n=1}^{\infty}\frac{1}{n}exp\left(-\frac{n^2\pi^2 n_x t}{x_e^2}\right)sin\frac{n\pi x_f}{2x_e}cos\frac{n\pi x_w}{x_e}cos\frac{n\pi x}{x_e}\right]$

References

[1] Fayers F. J., Arbabi S. and Aziz K., 1995. Challenges in reservoir engineering from prospects for horizontal wells. *Petroleum Geoscience*, Vol. 1, 1995, pp.13-23

[2] Escobar F. H., Muñoz O. F. and Sepúlveda J. A.. 2004. Horizontal Permeability Determination From The Elliptical Flow Regime Of Horizontal Wells. *CT&F Ciencia, Tecnología y Futuro*, diciembre, año/vol. 2, número 005 Instituto Colombiano del Petróleo Bucaramanga, Colombia pp. 83-95

[3] Moncada K., Tiab D., Escobar F. H., Montealegre M., Chacon A., Zamora R. and. Nese S-L. , 2005. Determination of Vertical and Horizontal Permeabilities for Vertical Oil and Gas Wells with Partial Completion and Partial Penetration using Pressure and Pressure Derivative Plots Without Type-Curve Matching. CT&F Ciencia, Tecnología y Futuro, vol. 3, núm. 1, diciembre, 2005, pp. 77-95 ECOPETROL S.A. Bucaramanga, Colombia.

[4] Li C., 2021. Production Analysis for Fractured Vertical Well in Coal Seam Reservoirs with Stimulated Reservoir Volume. Hindawi Geofluids Volume 2021, Article ID 1864734, 12 pages https://doi.org/10.1155/2021/1864734

[5] Agullera R. ; Michael C. Ng, 1991. Transient Pressure Analysis of Horizontal Wells in Anisotropic Naturally Fractured Reservoirs . *SPE Form Eval* 6 (01): 95–100. Paper Number: SPE-19002-PA. https://doi.org/10.2118/19002-PA

[6] Rbeawi S. A., Kadhim F. S., 2021. The Impact of Completion Technology on Flow Dynamics and Pressure Behaviors of Horizontal Wells. Iraqi Journal of Oil & Gas Research, Vol. 1, No. 1 (2021)

[7] Kuchuk F. J.; Goode P. A.; Wilkinson D. J.; Thambynayagam R. K. M.. 1991. Pressure-Transient Behavior of Horizontal Wells With and Without Gas Cap or Aquifer**.** *SPE Form Eval* 6 (01): 86–94. Paper Number: SPE-17413-PA. https://doi.org/10.2118/17413-PA

[8] Engler, T. W. and Tiab, D., 1996. "Analysis of pressure and pressure derivatives without type-curve matching. 6- Horizontal well tests in anisotropic reservoirs". *J. Pet. Sci. and Eng.*, 15 pp., 153-168.

[9] Sun, R.J., 1969. Theoretical size of hydraulically induced horizontal fractures and corresponding surface uplift in an idealized medium. J. Geophys. Res. 74 (25), 5995–6011.

[10] Chhina, H.S., Luhning, R.W., Bilak, R.A., Best, D.A., 1987. A horizontal fracture test in the Athabasca Oil Sands. In: PETSOC-87-38-56 Presented at the Annual Technical Meeting, Calgary, Alberta.

[11] Nicholl, M.J., Glass, R.J., 2001. Simulation of immiscible viscous displacement within the plane of a horizontal fracture. In: ARMA-01-0205 Presented at the 38th U.S. Symposium on Rock Mechanics. USRMS, Washington, DC.

[12] Smith, M.B., Montgomery, C., 2015. Hydraulic Fracturing. Crc Press.

[13] [13] Wright, C.A., Davis, E.J., Weijers, L., Minner, W.A., Hennigan, C.M., Golich, G.M., 1997. Horizontal hydraulic fractures: oddball occurrences or practical engineering concern? In: SPE 30230 Presented at SPE Western Regional Meeting, Long Beach, California.

[14] Gringarten A.C.; Ramey, Jr H.J..; Raghavan R.. 1975. Applied Pressure Analysis for Fractured Wells *J Pet Technol* 27 (07): 887–892. Paper Number: SPE-5496-PA. https://doi.org/10.2118/5496-PA

[15] Chu H. , Chen X. L., Z., Zhao X., Liu W., Dong P., 2019. Transient pressure analysis of a horizontal well with multiple, arbitrarily shaped horizontal fractures. Journal of Petroleum Science and Engineering. https://doi.org/10.1016/j.petrol.2019.06.003

[16] Odeh A. S. and Babu D.K. (1990): Transient Flow Behavior of Horizontal Wells: Pressure Drawdown and Buildup Analysis 'SPE Formation Evaluation, March, Pg 10-14.

[17] Goode, P. A. and Thambynayagam, R. K., 1987. "Pressure drawdown and buildup analysis of horizontal wells in anisotropic media". *SPE Formation Evaluation*, 683-697.

[18] Gringarten A.C., and Ramey H.J.J r, (1973): The use of Source and Green's Functions in solving Unsteady-flow Problems in Reservoirs. *Society of Petroleum Engineers Journal*, vol. 13, Pg.285-296.

[19] Mutisya M. P. , Adewole E. S., Awuor Kennedy, Otieno and Oyoo Daniel Okang. A Mathematical Model for Pressure Distribution in a Bounded Oil ReservoirSubject to Single-Edged and Bottom Constant Pressure. IOSR Journal of Mathematics (IOSR-JM). Volume 16, Issue 4 Ser. I (Jul.–Aug. 2020), PP 24-30. DOI: 10.9790/5728-1604012430.